1060 © *1983 The Chemical Society of Japan* *Bull. Chem. Soc. Jpn.*, **56**, *1060—1066 (1983)* [Vol. 56, No. 4

A Nuclear Magnetic Resonance Study of the Kinetics of Ligand Exchange Reactions in Uranyl Complexes. III. Dimethyl Sulfoxide Exchange in Bis(β-diketonato)(dimethyl sulfoxide)dioxouranium(VI)

Yasuhisa IKEDA, Hiroshi TOMIYASU, and Hiroshi FUKUTOMI*
Research Laboratory for Nuclear Reactors, Tokyo Institute of Technology, O-okayama, Meguro-ku, Tokyo 152

(Received September 30, 1982)

The exchange reactions of dimethyl sulfoxide (DMSO) with $UO_2(acac)_2dmso$ and $UO_2(dbm)_2dmso$ (acac= acetylacetonate, dbm=dibenzoylmethanate) have been studied by the NMR method in CD_3COCD_3 and CD_2Cl_2. In CD_3COCD_3, rates of DMSO exchange for these complexes are independent of the free DMSO concentrations. Rate constants (s^{-1}) at 25 °C and activation parameters $\Delta H^{\neq}$ ($kJ\ mol^{-1}$) and $\Delta S^{\neq}$ ($J\ K^{-1}\ mol^{-1}$) are 2.36×10^2, 45.8 ± 0.8, -46.6 ± 2.9 for $UO_2(acac)_2dmso$, and 3.92×10^2, 44.5 ± 0.4, -46.2 ± 2.1 for $UO_2(dbm)_2dmso$, respectively. In CD_2Cl_2, the exchange rates are dependent on the free DMSO concentration. For $UO_2(acac)_2dmso$, rate$=(k_d+k_IK_{OS}[DMSO])[UO_2(acac)_2dmso]/(1+K_{OS}[DMSO])$, where $k_d(25\ °C)=1.02\times10^2\ s^{-1}$, $\Delta H^{\neq}=47.9\pm5.2\ kJ\ mol^{-1}$, and $\Delta S^{\neq}=-46.6\pm11.2\ J\ K^{-1}\ mol^{-1}$, and $k_I(25\ °C)=1.01\times10^3\ s^{-1}$, $\Delta H^{\neq}=35.4\pm12.4\ kJ\ mol^{-1}$, and $\Delta S^{\neq}=-69.7\pm20.5\ J\ K^{-1}\ mol^{-1}$, and $K_{OS}(10\ °C)=4.6\pm2.1\ M^{-1}$ ($M=mol\ dm^{-3}$). For $UO_2(dbm)_2dmso$, rate$=(k_1+k_2[DMSO])\ [UO_2(dbm)_2dmso]$, where $k_1(25\ °C)=1.74\times10^2\ s^{-1}$, $\Delta H^{\neq}=29.6\pm2.2\ kJ\ mol^{-1}$, $\Delta S^{\neq}=-104\pm9\ J\ K^{-1}\ mol^{-1}$, and $k_2(25\ °C)=1.62\times10^3\ M^{-1}\ s^{-1}$, $\Delta H^{\neq}=34.9\pm0.6\ kJ\ mol^{-1}$, and $\Delta S^{\neq}=-67.2\pm2.4\ J\ K^{-1}\ mol^{-1}$. The D and I mechanisms are proposed for the DMSO exchange in these complexes.

Recently, the kinetics of the ligand exchange reactions for $UO_2L_n^{2+}$, where $n=4$ and L is water[1] or hexamethylphosphoric triamide (hmpa),[2] and $n=5$ and L is *N,N*-dimethylacetamide(dma),[3] trimethyl phosphate(tmp) and triethyl phosphate(tep),[4] dimethyl sulfoxide (dmso),[5] *N,N*-dimethylformamide(dmf),[6] and *N*-methylacetamide(nma),[7] have been studied by NMR. However, only a few studies have been concerned with ligand exchange in uranyl chelate complexes.[8,9] The uranyl β-diketonato complexes, $UO_2(\beta\text{-diketonato})_2L$ (L=adduct ligands), have been of particular interest among these chelate complexes in view of their role in the extraction of uranyl ions.[10–14]

This paper will deal with the kinetics of DMSO exchange in $UO_2(acac)_2dmso$ (acac=acetylacetonate) and $UO_2(dbm)_2dmso$ (dbm=dibenzoylmethanate) by NMR. At the same time the structure of these complexes will be determined, since it has not been reported whether the pentagonal bipyramidal structure which was found by the X-ray study of crystalline $UO_2(acac)_2$-H_2O[15,16] remains unchanged in solution.

Experimental

Synthesis of Complexes. The $UO_2(acac)_2dmso$ complex was prepared by dissolving $UO_2(acac)_2H_2O$ in warm DMSO. The $UO_2(acac)_2H_2O$ complex was prepared according to the procedure of Comyns *et al.*[17] The $UO_2(acac)_2dmso$ solution was cooled and the resultant orange crystals were filtered and dried *in vacuo* for 1 d. The $UO_2(dbm)_2dmso$ complex was prepared by mixing DMSO with diethyl ether solution of $UO_2(dbm)_2H_2O$ which was synthesized by mixing an aqueous solution of uranyl(VI) acetate dihydrate (1 mol) with an ethanolic solution of dibenzoylmethane (2 mol).[18] The resultant orange crystals were filtered, washed with diethyl ether and dried *in vacuo* for 1 d. The composition of these complexes was determined by elemental analysis. The results are as follows: Calcd for $UO_2(acac)_2dmso$: C, 26.38; H, 3.69%. Found: C, 26.49; H, 3.66%. Calcd for $UO_2(dbm)_2dmso$: C, 48.37; H, 3.55; S, 4.03%. Found: C, 48.32; H, 3.52; S, 4.08%. Elemental analysis of the complexes was carried out in the Institute of Physical and Chemical Research.

Other Materials. Acetone-d_6(CD_3COCD_3, Merck 99.8%) and dichloromethane-d_2 (CD_2Cl_2, Merck 99%), which were used as solvents, were dried over 3A and 4A molecular sieves (Wako Pure Chemical Ind. Ltd.), respectively. Dimethyl sulfoxide (Wako Pure Chemical Ind. Ltd.) was distilled *in vacuo*, followed by distillation with molecular sieves, and stored over 3A molecular sieves. Acetylacetone (Wako Pure Chemical Ind. Ltd.) was used without further purification.

Preparation of Samples. Sample solutions in the appropriate solvent were prepared by weighing sample substances in a 1 cm^3 volumetric flask and some of each solution was placed in an NMR sample tube and sealed. All samples were prepared in a glove box filled with dried nitrogen. Proper precautions were taken to minimize the probability of photochemical redox reactions.

Measurement of NMR and IR Spectra. The measurements of the ^1H NMR spectra were carried out at 100 MHz on a JEOL JNM-MH 100 NMR spectrometer and JEOL JNM-FX 100 FT-NMR spectrometer equipped with a JNM-VT-3B temperature controller. Infrared spectra of the $UO_2(acac)_2$-dmso complex in CD_3COCD_3 and CD_2Cl_2 were recorded in the 200—4000 cm^{-1} range by using a JASCO DS-701G IR spectrometer.

Kinetic Analysis. The kinetic parameters were calculated by using a program on the assumption of a two-site exchange process.[19] Input parameters for this program are the chemical shifts and the linewidths at half amplitude of each signal of the coordinated and free sites at −60 °C where no exchange was observed, the site populations, and appropriate life-times (τ-values). The experimental spectra are compared with the calculated spectra and the best-fit τ-values are determined. All computations were carried out with a Hitach M-200 computer.

Results and Discussion

The Structure of $UO_2(acac)_2dmso$ in Solutions. The ^1H NMR spectra in DMSO and CD_3COCD_3 mixtures including $UO_2(acac)_2dmso$ at −25 and 40 °C are shown in Fig. 1. In the spectrum at −25 °C, the signals of (a) and (d) can be assigned to be the methyl protons and 3-H protons of the coordinated acac, respectively. The signals (b) and (c) are the methyl

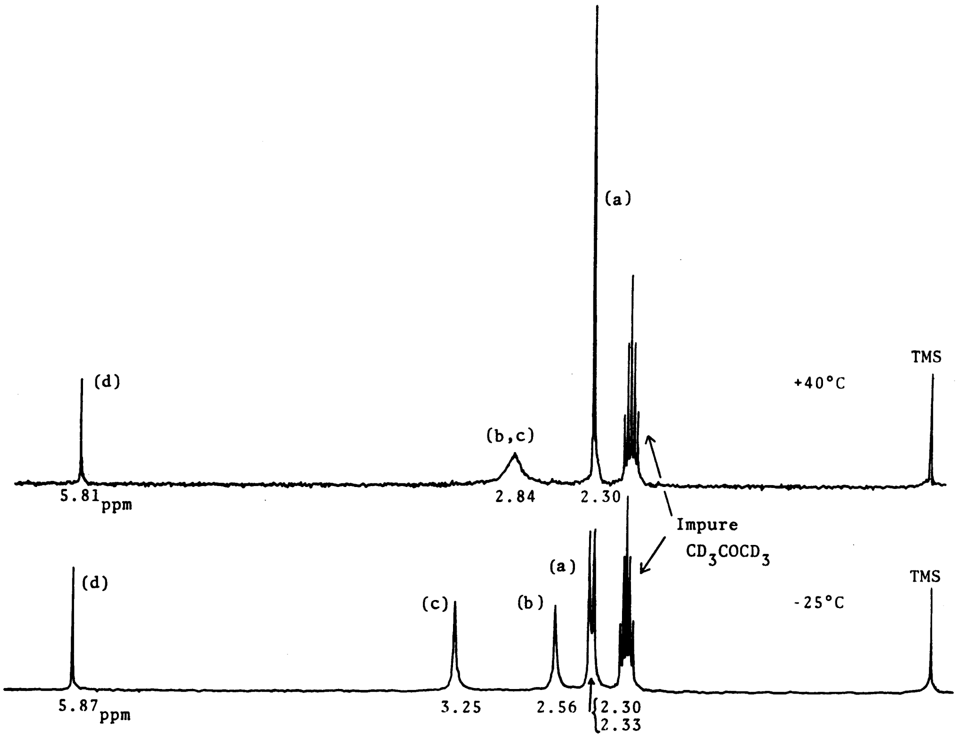

Fig. 1. ^{1}H NMR spectra of a solution consisting of $UO_2(acac)_2$dmso (0.0298 M), DMSO (0.0294 M), and CD_3COCD_3 (13.4 M) at −25 and 40 °C, respectively.

protons of the free and coordinated DMSO, respectively. A comparison of the integrated areas for (b) and (c) indicates that one DMSO molecule is coordinated to each uranyl ion. The area ratio of (a) to (c) to (d) was 6 : 3 : 1, the signal of (d) being used as a standard. The ratio was constant in solutions of various compositions. These facts indicate that two acetylacetonate ions and one DMSO molecule coordinate to uranyl ion. The separation of the methyl protons for coordinated acac means that these methyl groups are not geometrically identical. This may be explained by assuming the structure of this complex to be pentagonal bipyramidal like the crystal structure of the $UO_2(acac)_2H_2O$ complex,[15,16)] because in such a structure the methly protons of coordinated acac exist in two different magnetic circumstances, with one near and one distant from the coordinated DMSO. The fact that the 3-H proton of the coordinated acac has a single peak also supports the proposed structure. In CD_2Cl_2, similar phenomena were also obseved in the ^{1}H NMR spectra.

The IR measurements for $UO_2(acac)_2$dmso were made in CD_3COCD_3 and CD_2Cl_2. The results are given in Table 1. The S=O stretch of the uranyl complex in CD_3COCD_3 and CD_2Cl_2 is observed at 1010 cm^{-1}, which is 45 cm^{-1} lower than the 1055 cm^{-1} observed in pure DMSO. Cotton and Francis[20)] have shown that the S=O stretching frequency of sulfoxide in complexes decreases when coordination occurs through oxygen. Hence, it is concluded that one DMSO molecule is coordinated through oxygen in this complex. In addition, it was found that the two acetylacetonate ions were coordinated as bidentate ligands, because only one band corresponding to the carbonyl vibration was observed at frequencies less than 1600 cm^{-1}, which is the characteristic frequency of the carbonyl vibration for chelated metal β-diketone complexes.[21)]

TABLE 1. CHARACTERISTIC IR STRETCHING FREQUENCIES FOR $UO_2(acac)_2$dmso IN SOLUTION

Solvent	ν_3(O=U=O) cm^{-1}	ν(S=O) cm^{-1}	ν(C–O) cm^{-1}
CD_3COCD_3	905	1010	1517
CD_2Cl_2	908	1010	1570

The Structure of $UO_2(dbm)_2$dmso in Solutions. Figure 2 shows the ^{1}H NMR spectra of $UO_2(dbm)_2$dmso in DMSO and CD_3COCD_3 mixtures at −30 and 30 °C. At −30 °C, the signals (a) and (b) can be assigned to be the methyl protons of the free and coordinated DMSO, respectively. The signals (c) and (d) are the 3-H protons and the protons on benzene rings of the coordinated dbm, respectively. The area ratio of (d) to (c) to (b) was 10 : 1 : 3 and the ratio was constant in solutions of various composition. The signal for the 3-H protons of the coordinated dbm is a single peak as seen in Fig. 2. These ^{1}H NMR spectra in solutions containing $UO_2(dbm)_2$dmso indicate that two dibenzoylmethanate ions and one DMSO molecule coordinate to uranyl ion. Therefore, the structure of $UO_2(dbm)_2$dmso is presumed to be pentagonal bipyramidal which is the same as that of $UO_2(acac)_2$dmso.

DMSO Exchange in $UO_2(acac)_2$dmso. It is noted from Fig. 1 that DMSO exchanges between coordinated and free sites, because the methyl proton signals of the coordinated and free DMSO are observed at −25 °C, while only a single methyl proton signal for DMSO is observed at 40 °C. In addition, coalescence of the methyl proton signal for coordinated acac at 40 °C may

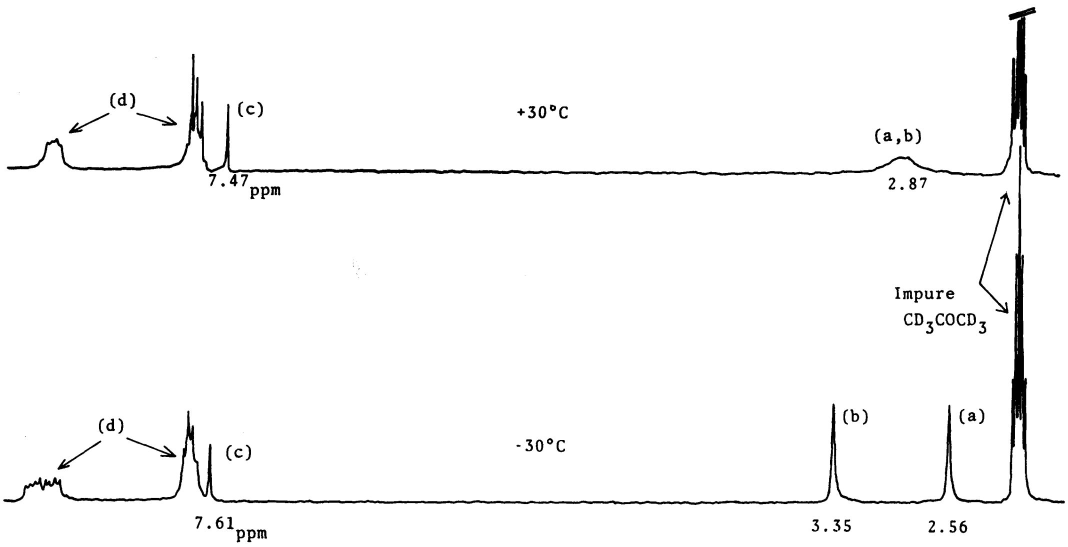

Fig. 2. ^{1}H NMR spectra of a solution consisting of $UO_2(dbm)_2dmso$ (0.0117 M), DMSO (0.0115 M), and CD_3COCD_3 (13.5 M) at −30 and 30 °C, respectively.

TABLE 2. SOLUTION COMPOSITION AND KINETIC PARAMETERS FOR THE EXCHANGE OF DMSO IN $UO_2(acac)_2$ dmso

Solution	$[UO_2(acac)_2dmso]$ / 10^{-2} M	$[DMSO]^{a)}$ / M	$[CD_3COCD_3]$ / M	$[CD_2Cl_2]$ / M	$\Delta H^{\ddagger}$ / kJ mol^{-1}	$\Delta S^{\ddagger}$ / J K^{-1} mol^{-1}	$k_{ex}(25\ °C)^{b)}$ / 10^2 s^{-1}
i	2.98	0.0294	13.4		45.8± 0.4	−44.9± 1.7	2.89
ii	4.65	0.151	13.2		45.8± 0.8	−46.6± 2.9	2.36
iii	4.58	0.243	13.2		39.5± 0.8	−68.9± 2.9	2.07
iv	4.70	0.321	13.0		41.6± 1.7	−60.5± 5.9	2.43
v	1.79	0.0282		15.7	k_d path		
vi	3.53	0.0320		15.6	47.9± 5.2	−46.6±11.2	1.02
vii	4.05	0.0563		15.4	k_I path		
viii	7.78	0.0870		15.4	35.4±12.4	−69.7±20.5	10.1
ix	10.5	0.239		14.5			

a) Added as DMSO. b) Calculated values from $\Delta H^{\ddagger}$ and $\Delta S^{\ddagger}$ at 25 °C.

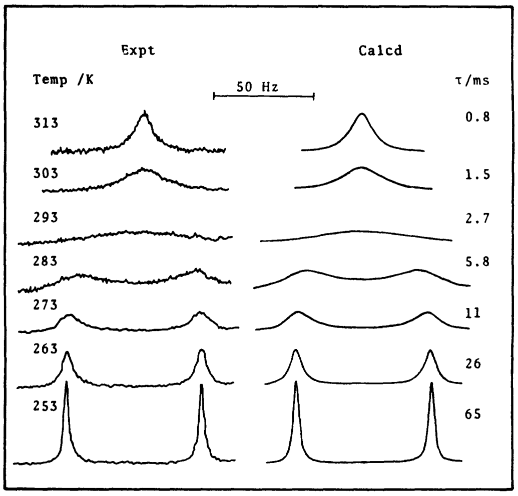

Fig. 3. Experimental (left side) and best-fit calculated lineshapes of a solution consisting of $UO_2(acac)_2dmso$ (0.0298 M), DMSO (0.0294 M), and CD_3COCD_3 (13.4 M). Temperatures and best-fit τ-values are shown at left and right sides of the figure, respectively.

be attributed to intermolecular DMSO exchange or intramolecular exchange for this complex.[22] The ^{1}H NMR measurements for DMSO methyl protons were carried out at various temperatures in order to examine in detail the change in lineshape. Results are shown in Fig. 3. The temperature dependence of the spectra is consistent with the results of previous work dealing with the DMSO exchange in $UO_2(dmso)_5^{2+}$.[5] The best-fit τ-values at each temperature were obtained by the method described in the Experimental Section. The calculated lineshapes are shown in Fig. 3 together with the corresponding best-fit τ-values.

The first-order rate constants, k_{ex}, for the DMSO exchange in $UO_2(\beta\text{-diketonato})_2dmso$ were calculated from the following equations:

$$\tau = \tau_c P_f = \tau_f P_c \tag{1}$$

$$k_{ex} = 1/\tau_c = \text{rate}/[UO_2(\beta\text{-diketonato})_2dmso] = (kT/h)\exp(-\Delta H^{\ddagger}/RT)\exp(\Delta S^{\ddagger}/R), \tag{2}$$

where the τ_c and τ_f are the mean life-times of the coordinated and free sites, respectively and P_c and P_f refer to the mole fractions of the coordinated and free DMSO, respectively. The rate constants, k_{ex}, were

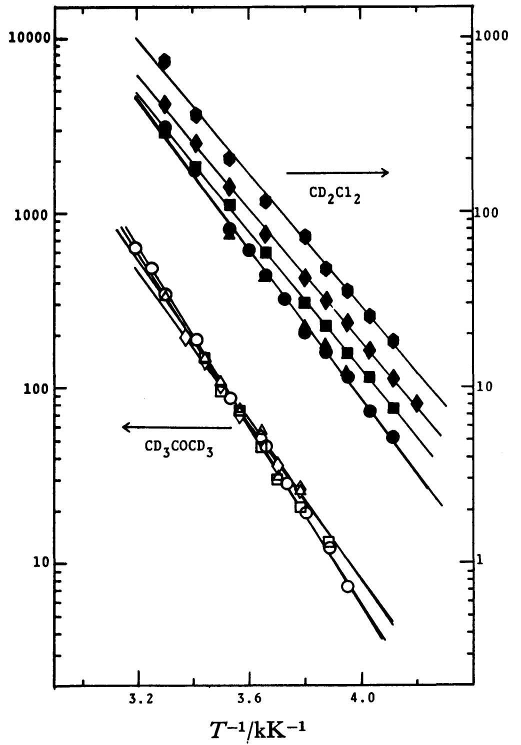

Fig. 4. Semilogarithmic plots of k_{ex} against the reciprocal temperature for the exchange of DMSO in $UO_2(acac)_2dmso$ in CD_3COCD_3 and CD_2Cl_2. The symbols of ○, △, □, ◇, ●, ▲, ■, ◆, and ⬮ correspond to i, ii, iii, iv, v, vi, vii, viii, and ix solutions in Table 2.

obtained for various solutions listed in Table 2. In Fig. 4, the values of k_{ex} are plotted semilogarithmically against the reciprocal temperature. The activation parameters obtained from Fig. 4 are listed in Table 2. It can be seen from Table 2 and Fig. 4 that the rates of DMSO exchange in CD_3COCD_3 are independent of the free DMSO, while those of the DMSO exchange in CD_2Cl_2 depend on the concentration of free DMSO. The values of k_{ex} in the CD_2Cl_2 system were plotted against the DMSO concentration as shown in Fig. 5. This figure indicates that the rate of DMSO exchange in CD_2Cl_2 does not obey a simple linear relationship with the DMSO concentration.

DMSO Exchange in $UO_2(dbm)_2dmso$. It can be also expected from Fig. 2 that the DMSO exchanges

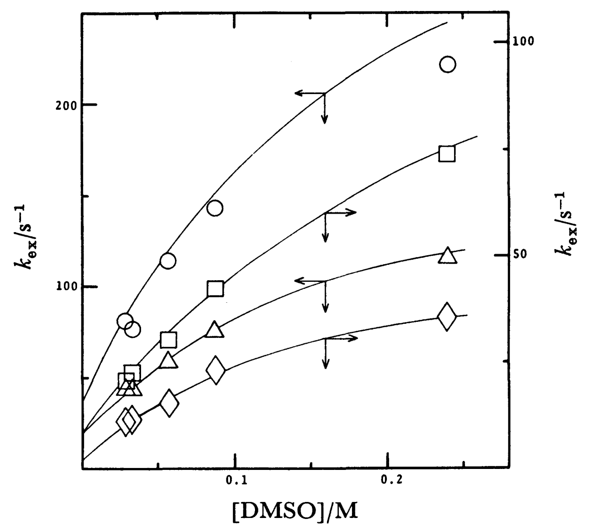

Fig. 5. Plots of k_{ex} *vs.* [DMSO] for the exchange of DMSO in $UO_2(acac)_2dmso$ in CD_2Cl_2. ○: 10 °C; △: 0 °C; □: −10 °C; ◇: −20°C.

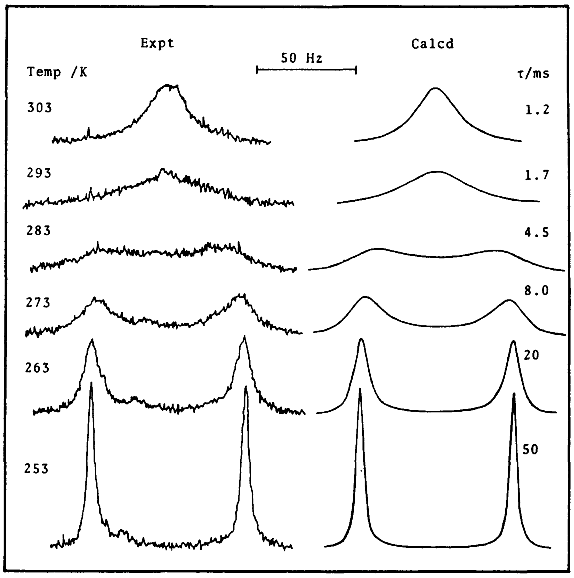

Fig. 6. Experimental (left side) and best-fit calculated lineshapes of a solution consisting of $UO_2(dbm)_2dmso$ (0.0117 M), DMSO (0.0115 M), and CD_3COCD_3 (13.5 M). Temperatures and best-fit τ-values are shown at left and right sides of the figure, respectively.

Table 3. Solution composition and kinetic parameters for the exchange of DMSO in $UO_2(dbm)_2dmso$

Solution	$[UO_2(dbm)_2dmso]$ / 10^{-2} M	[DMSO]^a) / M	$[CD_3COCD_3]$ / M	$[CD_2Cl_2]$ / M	$\Delta H^{\ne}$ / kJ mol^{-1}	$\Delta S^{\ne}$ / J K^{-1} mol^{-1}	k_{ex}(25 °C)^b) / 10^2 s^{-1}
i	1.17	0.0115	13.5		44.5±0.8	−47.9±2.5	3.37
ii	2.64	0.0384	13.3		44.5±0.4	−46.2±2.1	3.92
iii	3.10	0.0678	13.1		43.3±0.4	−50.8±2.1	3.68
iv	6.37	0.0627		14.8	k_1 path		
v	6.39	0.124		14.8	29.6±2.2	−104.2±8.6	1.74
vi	6.37	0.266		14.8	k_2 path		
vii	6.36	0.376		14.7	34.9±0.6	−67.2±2.4	16.2/M^{-1}
viii	6.31	0.499		14.7			

a) Added as DMSO. b) Calculated values from $\Delta H^{\ne}$ and $\Delta S^{\ne}$ at 25 °C.

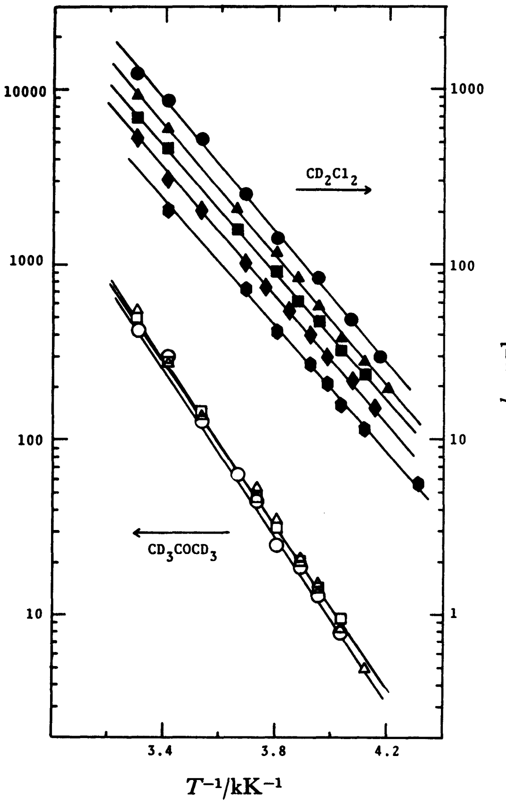

Fig. 7. Semilogarithmic plots of k_{ex} against the reciprocal temperature for the exchange of DMSO in $UO_2(dbm)_2dmso$ in CD_3COCD_3 and CD_2Cl_2. The symbols of ○, △, □, ⧫, ◆, ■, ▲, and ● correspond to i, ii, iii, iv, v, vi, vii, and viii solutions in Table 3.

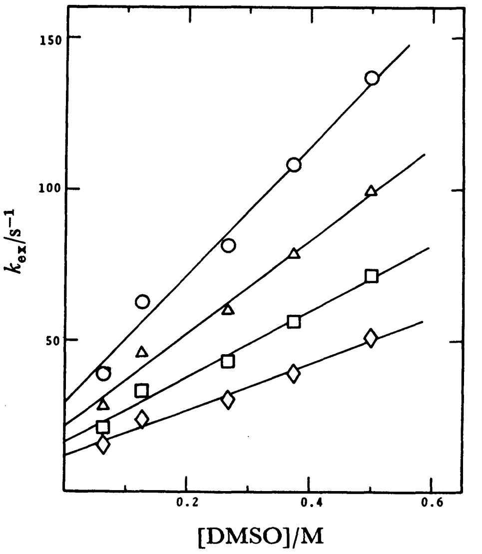

Fig. 8. Plots of k_{ex} vs. [DMSO] for the exchange of DMSO in $UO_2(dbm)_2dmso$ in CD_2Cl_2. ○: −10 °C; △: −15 °C; □: −20 °C; ◇: −25 °C.

between the coordinated and free sites with $UO_2(dbm)_2$-dmso in a DMSO and CD_3COCD_3 mixture, because the signal of the DMSO methyl protons changes from two signals at −30 °C to one signal at 30 °C. More detailed spectral changes with temperature are shown in Fig. 6 for the temperature region from −20 to 30 °C.

TABLE 4. THE VALUES OF k_1 AND k_2 AT VARIOUS TEMPERATURES FOR THE EXCHANGE OF DMSO IN $UO_2(dbm)_2dmso$ IN CD_2Cl_2

Temp / °C	k_1 / $10\ s^{-1}$	k_2 / $10^2\ M^{-1}\ s^{-1}$
−10	2.91±0.44	2.12±0.14
−15	2.18±0.33	1.53±0.11
−20	1.62±0.25	1.09±0.08
−25	1.19±0.18	0.76±0.06

The coalescence of the coordinated and free DMSO signals was also observed at high temperature. The best-fit τ-values at each temperature were determined by the same method as mentioned before and the calculated lineshapes are also shown in Fig. 6. The first-order exchange rate constants, k_{ex}, were calculated by Eqs. 1 and 2. The k_{ex} values obtained for the solutions listed in Table 3 were plotted semilogarithmically against the reciprocal temperature (Fig. 7). The activation parameters are given in Table 3. As can be seen in Fig. 7 and Table 3, the rate of DMSO exchange in CD_3COCD_3 is independent of the free DMSO concentration, while the rate in CD_2Cl_2 is dependent on the concentration of free DMSO. A plot of k_{ex} values which were obtained in CD_2Cl_2 against the free DMSO concentration is linear (Fig. 8) and results in the following equation.

$$k_{ex} = k_1 + k_2[\mathrm{DMSO}] \tag{3}$$

The values of k_1 and k_2 were, respectively, obtained from the intercepts and the slopes of the plots from Fig. 8 by means of the least-squares method, and are shown in Table 4. The activation parameters for these paths are given in Table 3.

Possible Mechanism. It was found that the rate of the DMSO exchange reactions in $UO_2(acac)_2dmso$ and $UO_2(dbm)_2dmso$ in CD_3COCD_3 is independent of the free DMSO. This fact suggests that the DMSO exchange process for these complexes in CD_3COCD_3 proceeds through either the D or the I mechanism.[23]

In the D mechanism, the exchange process is expressed as

$$\mathrm{UO_2(\beta\text{-diketonato})_2dmso + DMSO^*} \xrightarrow[\text{slow}]{k_d}$$
$$\mathrm{UO_2(\beta\text{-diketonato})_2 + DMSO + DMSO^*} \xrightarrow[\text{fast}]{}$$
$$\mathrm{UO_2(\beta\text{-diketonato})_2dmso^* + DMSO.} \tag{4}$$

In this mechanism, the rate-determining step is the dissociation of the coordinated DMSO from $UO_2(\beta$-diketonato$)_2$dmso and an intermediate of reduced coordination number, $UO_2(\beta$-diketonato$)_2$, is formed. Thus, k_{ex} is given as

$$k_{ex} = k_d. \tag{5}$$

In the I mechanism, overall processes are represented as

$$\mathrm{UO_2(\beta\text{-diketonato})_2dmso + DMSO^*} \underset{\text{fast}}{\overset{K_{os}}{\rightleftharpoons}}$$
$$\mathrm{UO_2(\beta\text{-diketonato})_2dmso\cdots DMSO^*} \xrightarrow[\text{slow}]{k_i}$$

$$UO_2(\beta\text{-diketonato})_2dmso^{*}\cdots DMSO \xrightarrow[\text{fast}]{} UO_2(\beta\text{-diketonato})_2dmso^{*} + DMSO, \qquad (6)$$

where K_{os} is the formation constant of the outer-sphere complex, $UO_2(\beta\text{-diketonato})_2dmso\cdots DMSO^{*}$, and k_I is the interchange rate constant between DMSO molecules in the first coordination sphere and those in the second coordination sphere. Since the rate-determining step is the k_I path, k_{ex} is given by Eq. 7.

$$k_{ex} = k_I K_{os}[DMSO]/(1+K_{os}[DMSO]) \qquad (7)$$

If $K_{os}[DMSO] \gg 1$, Eq. 7 can be simplified as $k_{ex}=k_I$ and the exchange rate of DMSO becomes independent of DMSO. This mechanism also appears to be compatible with the results of the DMSO exchange in $UO_2(acac)_2dmso$ and $UO_2(dbm)_2dmso$ in CD_3COCD_3.

Although the D or I mechanism can not be distinguished by the form of the rate law, the I mechanism seems to be unlikely for the following reasons. In the I mechanism, the condition $K_{os}[DMSO] \gg 1$ is required and hence $K_{os} \gg 100\ M^{-1}$ should be satisfied over the concentration range in the present experiments. However, such a value of $K_{os}(\gg 100\ M^{-1})$ is too large considering the normal association constant between uncharged molecules. The D mechanism, on the other hand, might be supported by the fact that some uranyl complexes, *e.g.* $UO_2(H_2O)_4^{2+}$ [1,24,25] $UO_2(hmpa)_4^{2+}$ [2,26] exist in solution as a tetragonal bipyramid.

Another mechanism, where the rate-determining step is the ring-opening of one of the coordinated acac groups, might be proposed. However, this mechanism can be ruled out since the rate constant for ring-opening is about 2.04 s^{-1} at 25 °C in $o\text{-}C_6H_4Cl_2$ [27] which is much smaller than that observed for the DMSO exchange reaction.

For the DMSO exchange reaction for $UO_2(acac)_2$-dmso in CD_2Cl_2, the observed first-order rate constants, k_{ex}, depend on the free DMSO concentrations but not linearly as shown in Fig. 5. This fact might suggest that the DMSO exchange in this system proceeds through both the D and I mechanisms. From Eqs. 4 and 6, k_{ex} is given by Eq. 8.

$$k_{ex} = \frac{k_d + k_I K_{os}[DMSO]}{1+K_{os}[DMSO]} \qquad (8)$$

If $K_{os}[DMSO] \ll 1$, Eq. 8 can be simplified as $k_{ex}=k_d+k_I K_{os}[DMSO]$. This corresponds to the region of low DMSO concentration in Fig. 8, where k_{ex} changes linearly with DMSO concentration. If $K_{os}[DMSO] \gg 1$, k_{ex} is close to k_I. This is consistent with the fact that the k_{ex} values approach the limiting values at high DMSO concentrations. The values of k_d, k_I, and K_{os} were calculated by using the nonlinear least-squares method for Eq. 8 and are listed in Table 5. The experimental data are in close agreement with the calculated best-fit lines, which are shown in Fig. 5 as solid lines. The activation parameters for k_d and k_I were obtained from the data for various temperatures and are shown in Table 2.

TABLE 5. THE VALUES OF k_d, k_I, AND K_{os} AT VARIOUS TEMPERATURES FOR THE EXCHANGE OF DMSO IN $UO_2(acac)_2$ dmso IN CD_2Cl_2

Temp / °C	k_d / s^{-1}	k_I / $10^2\ s^{-1}$	K_{os} / M^{-1}
10	35.5±6.1	4.47±1.17	4.6±2.1
0	18.5±0.8	1.86±0.45	5.9±0.4
−10	8.38±0.44	1.65±0.08	3.1±0.2
−20	2.85±0.67	0.57±0.01	6.2±0.5

As can be seen in Fig. 8, the DMSO exchange in $UO_2(dbm)_2dmso$ behaves similar to that observed for $UO_2(acac)_2dmso$ in CD_2Cl_2 except for the plots being linear even at the high DMSO concentration range. In spite of the linear relationship of k_{ex} against the DMSO concentration, the A mechanism[23] seems to be unlikely, because the size of dbm is much larger than that of acac and the associative attack of the DMSO molecule should be sterically restricted for the dbm complex. If a similar mechanism (combination of the D and I mechanisms) as proposed for $UO_2(acac)_2dmso$ In CD_2Cl_2 is assumed, the condition of $K_{os}[DMSO] \ll 1$ should be satisfied over the range of DMSO concentrations from 0.0627 to 0.499 M. This means that K_{os} for $UO_2(dbm)_2dmso$ and DMSO is at least fivefold smaller than that between $UO_2(acac)_2dmso$ and DMSO. Considering the bulky size of dbm compared with that of acac, such a value of K_{os} might be expected to be reasonable.

The difference in exchange processes which were observed in two different solvents, CD_3COCD_3 and CD_2Cl_2, may primarily be attributed to the difference in affinity of these solvents for uranyl complexes. Acetone has a relatively large basicity compared with dichloromethane on the basis of Gutmann's donor number[28] and tends to solvate the second coordination spheres of uranyl complexes under the present experimental conditions. It may be predicted that in the case of DMSO exchange in CD_3COCD_3, solvation by CD_3COCD_3 assists the dissociation of DMSO from the first coordination sphere, instead of the free DMSO in the bulk solvent being involved in the activated complex. The dielectric constant of acetone (20.7) is larger than that of dichloromethane (8.93), and hence smaller K_{os} values are expected in CD_3COCD_3 than in CD_2Cl_2.

TABLE 6. KINETIC PARAMETERS FOR THE EXCHANGE OF DMSO IN VARIOUS URANYL COMPLEXES IN CD_3COCD_3

Complex	Mechanism	$\Delta H^{\ast}$ / kJ mol^{-1}	$\Delta S^{\ast}$ / J K^{-1} mol^{-1}	k_{ex}(25 °C) / s^{-1}
$UO_2(dmso)_5^{2+}$	D	53.8±2.4	6.3±14.5	5.53×10^3
	A	39.1±1.7	−28.1± 5.0	$3.22\times10^4/M^{-1}$
$UO_2(acac)_2$ dmso	D	45.8±0.8	−46.6± 2.9	2.36×10^2
$UO_2(dbm)_2$ dmso	D	44.5±0.4	−46.2± 2.1	3.92×10^2

Nevertheless, much larger values of k_{ex} in CD_3COCD_3 may support the above solvent assisted mechanism.

In spite of the DMSO exchange reactions in $UO_2(acac)_2dmso$ and $UO_2(dbm)_2dmso$ proceeding through the D and I mechanisms, large negative activation entropies are observed. This may be due to the solvent effect as suggested by Bennetto and Caldin.[29,30] They suggested that even though the exchange reaction proceeds dissociatively, $\Delta S^{\neq}$ may have negative values from the contribution of the solvent rearrangement around the metal complexes.

It is interesting to compare the DMSO exchange reactions in $UO_2(dmso)_5{}^{2+}$, $UO_2(acac)_2dmso$, and $UO_2(dbm)_2dmso$. The kinetic parameters of these DMSO exchange reactions in CD_3COCD_3 are summerized in Table 6. In the case of $UO_2(dmso)_5{}^{2+}$, the exchange rate is much faster than for the other complexes. This is consistent with general expectation that if the exchange reaction proceeds through an associative process, the reaction rate should be reduced significantly with crowding at the reaction site. It is quite reasonable that the bulky chelating ligands, acac and dbm, may hinder the approach of free DMSO to the first coordination sphere of the uranyl complex. This result may support the notion that the A mechanism is the major process for $UO_2(dmso)_5{}^{2+}$ in contrast with the D type processes for $UO_2(acac)_2dmso$ and $UO_2(dbm)_2dmso$.

The authors wish to thank Professor Gilbert Gordon of Miami University and Professor Thomas W. Swaddle of the University of Calgary for their helpful discussions.

References

1) Y. Ikeda, S. Soya, H. Tomiyasu, and H. Fukutomi, *J. Inorg. Nucl. Chem.*, **41**, 1333 (1979).

2) G. J. Honan, S. F. Lincoln, and E. H. Williams, *Inorg. Chem.*, **17**, 1855 (1978).

3) R. P. Bowen, S. F. Lincoln, and E. H. Williams, *Inorg. Chem.*, **15**, 2126 (1976).

4) J. Crea, R. Digiusto, S. F. Lincoln, and E. H. Williams, *Inorg. Chem.*, **16**, 2825 (1977).

5) Y. Ikeda, H. Tomiyasu, and H. Fukutomi, *Bull. Res. Lab. Nucl. Reactors.*, **4**, 47 (1979).

6) R. P. Bowen, G. J. Honan, S. F. Lincoln, T. M. Spotswood, and E. H. Williams, *Inorg. Chim. Acta*, **33**, 235 (1979).

7) G. J. Honan, S. F. Lincoln, and E. H. Williams, *J. Chem. Soc., Dalton Trans.*, **1979**, 1220.

8) A. Vasilescu, *Rev. Roum. Chim.*, **20**, 951 (1975).

9) K. Bokolo, J. J. Delpuech, L. Rodehüsen, and P. R. Rubini, *Inorg. Chem.*, **20**, 992 (1981).

10) T. V. Healy, D. F. Peppard, and G. W. Mason, *J. Inorg. Nucl. Chem.*, **24**, 1429 (1962).

11) T. V. Healy and J. R. Ferraro, *J. Inorg. Nucl. Chem.*, **24**, 1449 (1962).

12) Y. Baskin and J. R. Ferraro, *J. Inorg. Nucl. Chem.*, **30**, 241 (1968).

13) M. S. Subramanian and A. Viswanatha, *J. Inorg. Nucl. Chem.*, **31**, 2575 (1969).

14) J. M. Haigh and D. A. Thornton, *J. Inorg. Nucl. Chem.*, **33**, 3001 (1971).

15) E. Frasson, G. Bombieri, and C. Panattoni, *Nature*, **202**, 1325 (1964).

16) E. Frasson, G. Bombieri, and C. Panattoni, *Coord. Chem. Rev.*, **1**, 145 (1966).

17) A. E. Comyns, B. M. Gatehouse, and E. Wait, *J. Chem. Soc.*, **1958**, 4655.

18) L. Sacconi and G. Giannoni, *J. Chem. Soc.*, **1944**, 2368.

19) E. L. Eliel and N. L. Allinger, *Top. Stereochem.*, **3**, 97 (1968).

20) F. A. Cotton and R. Francis, *J. Am. Chem. Soc.*, **82**, 2986 (1960).

21) K. Nakamoto, "Infrared and Raman Spectra of Inorganic and Coordination Compounds," John Wiley and Sons, Inc., New York (1978).

22) Y. Ikeda, H. Tomiyasu, and H. Fukutomi, 3rd Symposium on Solution Chemistry, Tokyo, Oct. 1980, Abstr. p. 213.

23) C. H. Langford and H. B. Gray, "Ligand Substitution Processes," Benjamin, London (1974).

24) A. Fratiello, V. Kubo, R. E. Lee, and R. E. Schuster, *J. Phys. Chem.*, **74**, 3726 (1970).

25) A. Fratiello, V. Kubo, and R. E. Schuster, *Inorg. Chem.*, **10**, 744 (1971).

26) A. Fratiello, G. A. Vidlich, C. Cheng, and V. Kubo, *J. Solution Chem.*, **1**, 433 (1972).

27) Y. Ikeda, H. Tomiyasu, and H. Fukutomi, 30th Symposium on Coordination Chemistry, Tokyo, Oct. 1980, Abstr. p. 56.

28) V. Gutmann and R. Schmid, *Coord. Chem. Rev.*, **12**, 263 (1974).

29) H. P. Bennetto and E. F. Caldin, *J. Chem. Soc., A*, **1971**, 2198.

30) E. F. Caldin and H. P. Bennetto, *J. Solution Chem.*, **2**, 217 (1973).